nature genetics

SOX3 is required during the formation of the hypothalamo-pituitary axis

Karine Rizzoti[1,5], Silvia Brunelli[1,4,5], Danielle Carmignac[2], Paul Q Thomas[3], Iain C Robinson[2] & Robin Lovell-Badge[1]

The pituitary develops from the interaction of the infundibulum, a region of the ventral diencephalon, and Rathke's pouch, a derivative of oral ectoderm. Postnatally, its secretory functions are controlled by hypothalamic neurons, which also derive from the ventral diencephalon. In humans, mutations affecting the X-linked transcription factor SOX3 are associated with hypopituitarism and mental retardation, but nothing is known of their etiology. We find that deletion of *Sox3* in mice leads to defects of pituitary function and of specific central nervous system (CNS) midline structures. Cells in the ventral diencephalon, where *Sox3* is usually highly expressed, have altered properties in mutant embryos, leading to abnormal development of Rathke's pouch, which does not express the gene. Pituitary and hypothalamic defects persist postnatally, and SOX3 may also function in a subset of hypothalamic neurons. This study shows how sensitive the pituitary is to subtle developmental defects and how one gene can act at several levels in the hypothalamic-pituitary axis.

The development of complex organs composed of different cell types frequently depends on reciprocal induction events occurring between distinct tissue layers that lie adjacent to one another in the embryo. The pituitary is a well studied case in point. It originates from two ectoderm-derived tissues, with the posterior lobe developing from an evagination of the ventral diencephalon, the infundibulum, and the intermediate and anterior lobes deriving from Rathke's pouch, an invaginating domain in the roof of the oral ectoderm[1]. In the mature gland, the posterior lobe contains axon terminal projections from two populations of hypothalamic neuroendocrine neurons. The anterior and intermediate lobes contain several different endocrine cell types whose proliferation, hormone synthesis and secretion are regulated by factors secreted from hypothalamic neuroendocrine neurons.

During early development the infundibulum has an inductive role in the formation of the pituitary. For example, the genetic ablation of this domain in *Titf1*-null mice results in the complete absence of the pituitary gland[2]. The essential signaling molecules made by the infundibulum are thought to be FGF8 and BMP4, as both are necessary to induce early development of Rathke's pouch. FGF and BMP signals are also required to control the pattern of differentiation of cell types derived from Rathke's pouch[3,4].

Even subtle mutations that affect signaling pathways during early organogenesis can have profound effects on subsequent development and specification of mature cell types. These could arise in genes encoding the signaling molecules or their receptors, in transcription factors responsible for their expression or in genes required to specify the interacting tissues. In humans, SOX3, an HMG box protein (for review see ref. 5), is implicated in a syndrome of X-linked hypopituitarism and mental retardation[6]. In a single family whose males were deficient in growth hormone, a mutation in *SOX3* was identified. The consequences of this mutation on the function of the protein are not known. X-chromosome deletions encompassing *SOX3* are linked to several syndromes in humans, including mental retardation, but defects in pituitary function have not been reported[7,8].

SOX3 is a single-exon gene on the X chromosome in all mammals and is thought to be the gene from which *SRY*, the Y-linked testis determining gene, evolved[9,10]. Based on sequence homology, however, *SOX3* is more closely related to *SOX1* and *SOX2* (refs. 5,11). Together they comprise the *SOXB1* subfamily and are coexpressed throughout the developing CNS[11–13]. To study the role of *Sox3*, we targeted null mutations in the gene into XY embryonic stem (ES) cells, but injection of these cells into blastocysts resulted in early lethality of the chimeras due to a gastrulation defect (M. Parsons, C. Wise, S.B., M. Cohen-Tannoudji, K.R., L. Pevny & R.L.-B., unpublished data).

Therefore, to access later functions of *SOX3*, we initiated experiments using a conditional targeting strategy. In contrast to the chimera experiments in which the targeted ES cells were from an inbred mouse strain (129Sv/Ev), mice with deletions of *Sox3* were viable on outbred genetic backgrounds. *Sox3*-null mice have a range of phenotypes, including craniofacial abnormalities and reduced size and fertility. Because of the association between growth hormone deficiency and *SOX3* mutations in humans, we focused our investigations on the role of *Sox3* in pituitary development. We show here that *Sox3* is required in the presumptive hypothalamus and infundibulum

[1]Division of Developmental Genetics and [2]Division of Molecular Neuroendocrinology, MRC National Institute for Medical Research, The Ridgeway, Mill Hill, London NW7 1AA, UK. [3]Murdoch Children's Research Institute, Royal Children's Hospital, Melbourne, VIC 3052, Australia. [4]Present address: Stem Cell Research Institute, DIBIT-HSR, via Olgettina 58, 20132 Milan, Italy. [5]These authors contributed equally to this work. Correspondence should be addressed to R.L.-B. (rlovell@nimr.mrc.ac.uk).

Published online 15 February 2004; doi:10.1038/ng1309

for correct morphogenesis of Rathke's pouch and later for correct function of the hypothalamic-pituitary axis.

RESULTS

Targeted disruption of *Sox3*

To generate a *Sox3* conditional allele, we used homologous recombination in XY ES cells (the 129Sv/Ev line, AB1) to replace the coding region with a construct containing the *Sox3* open reading frame flanked by *lox*P sites (**Fig. 1a**). We inserted a marker gene encoding green fluorescent protein (GFP)[14] downstream to allow expression of GFP driven by *Sox3* regulatory sequences on Cre-mediated recombination (**Fig. 1a,d**).

Five independent ES cell colonies were correctly targeted, and two of these gave germline transmission from chimeric mice. We verified the presence of the conditional allele, $Sox3^{flox.gfp}$ (flox indicates flanked by *lox*P sites), by Southern-blot analysis (**Fig. 1b**). To generate mice with a deletion of *Sox3*, we bred females carrying $Sox3^{flox.gfp}$ with transgenic males carrying a β-actin–Cre construct conferring widespread Cre expression[15]. We confirmed the presence of the Cre-recombined allele, $Sox3^{\Delta gfp}$, by Southern-blot analysis (**Fig. 1b**) and by PCR (**Fig. 1c**). As expected, mutant XY embryos obtained from these matings showed no *Sox3* expression by *in situ* hybridization (data not shown) but expressed GFP in a pattern consistent with that of *Sox3* (**Fig. 1d**)[11,12]. Despite the complete absence of *Sox3*, we obtained live-born XY hemizygous null and XX heterozygous mice.

Phenotype of $Sox3^{\Delta gfp}$ mice

Null mutant males had a variable phenotype. Approximately one-third appeared normal, whereas the most seriously affected mice (**Fig. 1e**), which had poor growth and general weakness, did not survive to weaning. They also had craniofacial defects, including absence or abnormal shape and position of the pinna and overgrowth of teeth (K.R., unpublished data). Because *Sox3* is X-linked, heterozygous females are necessarily mosaic with respect to the mutation. Some had mild craniofacial defects, but they otherwise appeared normal. We bred these females with the less severely affected mutant males to generate homozygous mutant females and to maintain the $Sox3^{\Delta gfp}$ mutation.

Genotypes of progeny arising from intercrosses between heterozygous mutant females and hemizygous males did not deviate substantially from a normal mendelian distribution when we collected embryos between 8.5 and 15.5 days post coitum (d.p.c.; **Fig. 2**), but ~43% of mutant mice did not survive to weaning (**Fig. 2**). The sex ratio of the mutant mice did not deviate from normal. *Sox3* might have a role in sex determination as a repressor of male development[16], but we never observed any evidence for testicular development in homozygous mutant XX embryos at any stage. Therefore, *Sox3*, at least on this outbred genetic background, is not required for sex determination.

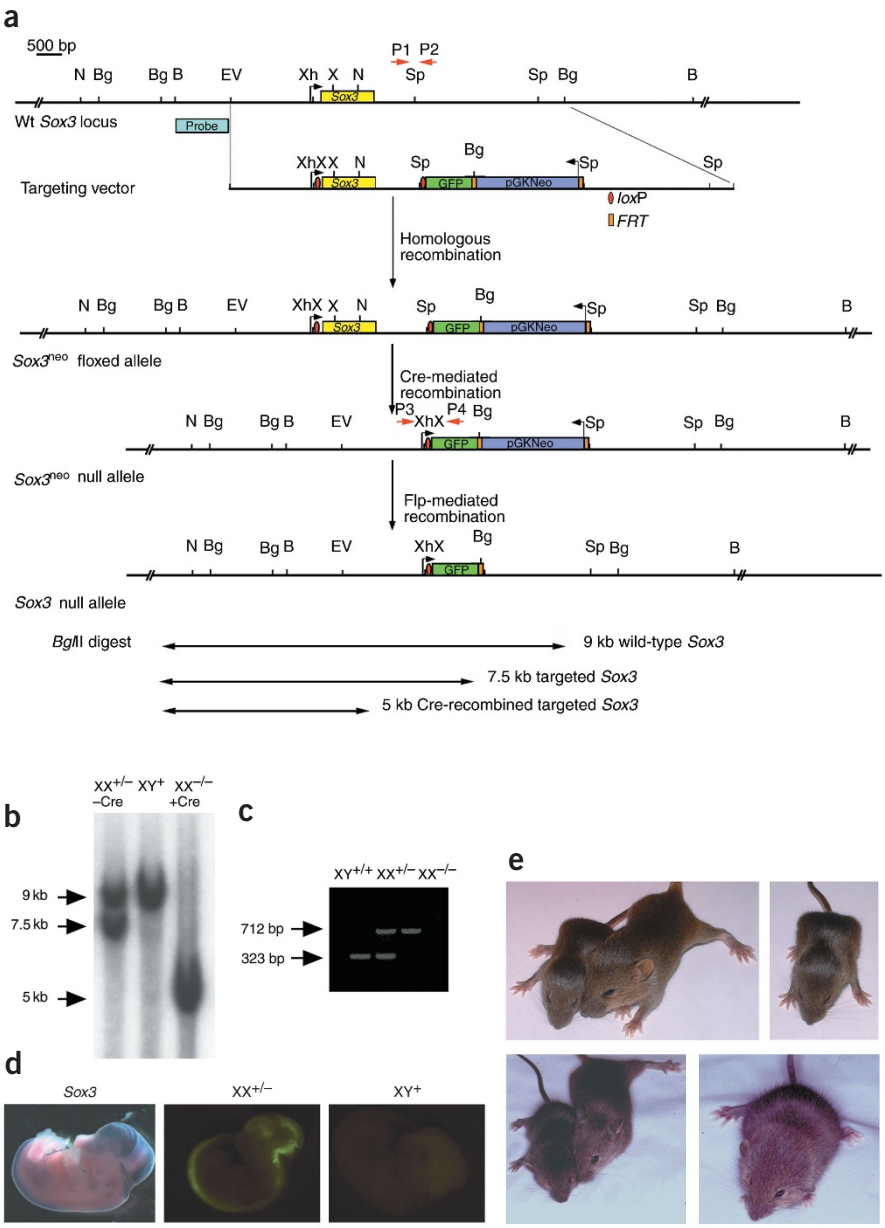

Figure 1 Conditional targeted inactivation of *Sox3*. (**a**) Structure of the mouse *Sox3* locus, targeting vector and recombinant alleles. The position of the primers used to genotype the wild-type (P1-P2) and $Sox3^{\Delta gfp}$ alleles (P3-P4) are indicated by arrowheads. (**b**) Southern-blot analysis of tail biopsies digested by *Bgl*II and hybridized with the 5′ genomic probe showing the expected fragments of 9 kb, 7.5 kb and 5 kb corresponding to the wild-type, $Sox3^{flox.gfp}$ and $Sox3^{\Delta gfp}$ alleles, respectively (see also **a**). (**c**) Genotyping of *Sox3* wild-type ($XY^{+/+}$), heterozygous ($XX^{+/-}$) and homozygous null ($XX^{-/-}$) mice by PCR amplification. The amplification product of 323 bp (using primers P1-P2) is specific to the wild-type *Sox3* 3′ untranslated region, and the product of 712 bp (using primers P3-P4) represents the $Sox3^{\Delta gfp}$ allele. (**d**) The live GFP activity domain in a 12.5-d.p.c. heterozygous ($XX^{+/-}$) embryo was absent in a wild-type (XY^{+}) embryo, but it matched the area of normal *Sox3* expression by *in situ* hybridization (for *Sox3*). (**e**) Upper panel: a pair of 2-week-old *Sox3*-null littermates showing the variability of the phenotype. Bottom panel: a 3-week-old *Sox3*-null mouse (right) showing craniofacial asymmetry and growth defects, together with a wild-type littermate (left).

Although we did not observe any reduction of fertility in the less severely affected mice, histological examination of testes from the most severely affected males showed considerable abnormalities with some necrotic, empty tubules (**Fig. 3a**,**b**), and the ovaries of the most severely affected homozygous females were small, with a high incidence of atretic follicles (**Fig. 3c**,**d**). *Sox3* is expressed in the adult testis in both humans and mice[7,11]. The protein was detected in mice in a subset of spermatogonia (**Fig. 3e–j**), probably type A (**Supplementary Fig. 1** online). The absence of SOX3 during this specific phase of germ cell development could explain the abnormal testes phenotype, but we observed no staining for SOX3 in ovaries (data not shown). It is therefore possible that the defects in both testes and ovaries, together with the growth defects seen in these mice, could be explained by pituitary deficiencies. Testes of younger mice (**Supplementary Fig. 1** online) were normal, consistent with a pituitary defect[17].

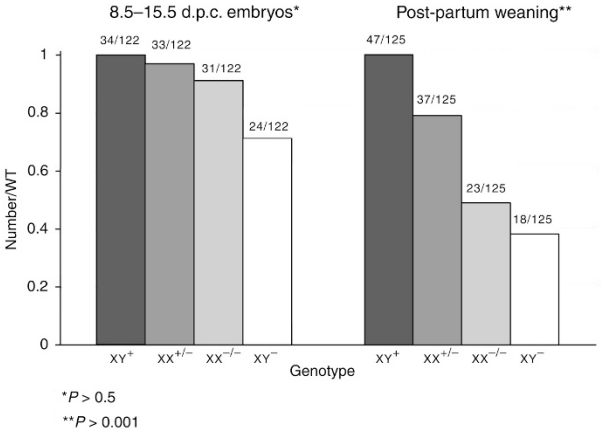

Figure 2 Genotypes of offspring obtained from *Sox3*$^{\Delta gfp}$ heterozygous (XX$^{+/-}$) and hemizygous (XY^{-}) intercrosses.

The pituitary gland is affected in *Sox3* mutants

We measured concentrations of pituitary growth hormone, follicle-stimulating hormone (FSH), luteinizing hormone and thyroid-stimulating hormone (TSH) in 2-month-old *Sox3* mutant and wild-type male littermates. The *Sox3* mutant mice had substantially lower concentrations (about three times lower on average) of pituitary growth hormone than did wild-type littermates (**Fig. 3k**). Concentrations of luteinizing hormone, FSH and TSH were also lower. These endocrine deficits varied between individual mice and correlated with body weight (**Fig. 3l**). The range of growth hormone deficits could easily account for the variable post-weaning growth rates in the moderately affected mutant mice[18], although the reduction in TSH could also contribute to this. Moreover, the reduction in gonadotrophins, either directly from a pituitary defect or as a secondary consequence of lower TSH levels, could contribute to the gonadal abnormalities.

Pituitary sections from wild-type mice immunostained for growth hormone showed clearly demarcated posterior, intermediate and anterior lobes, with heavy staining for growth hormone–producing somatotrophs (**Fig. 3m**,**n**). Except at the margins, the anterior lobe was separated from intermediate lobe cells by a single pituitary cleft, the

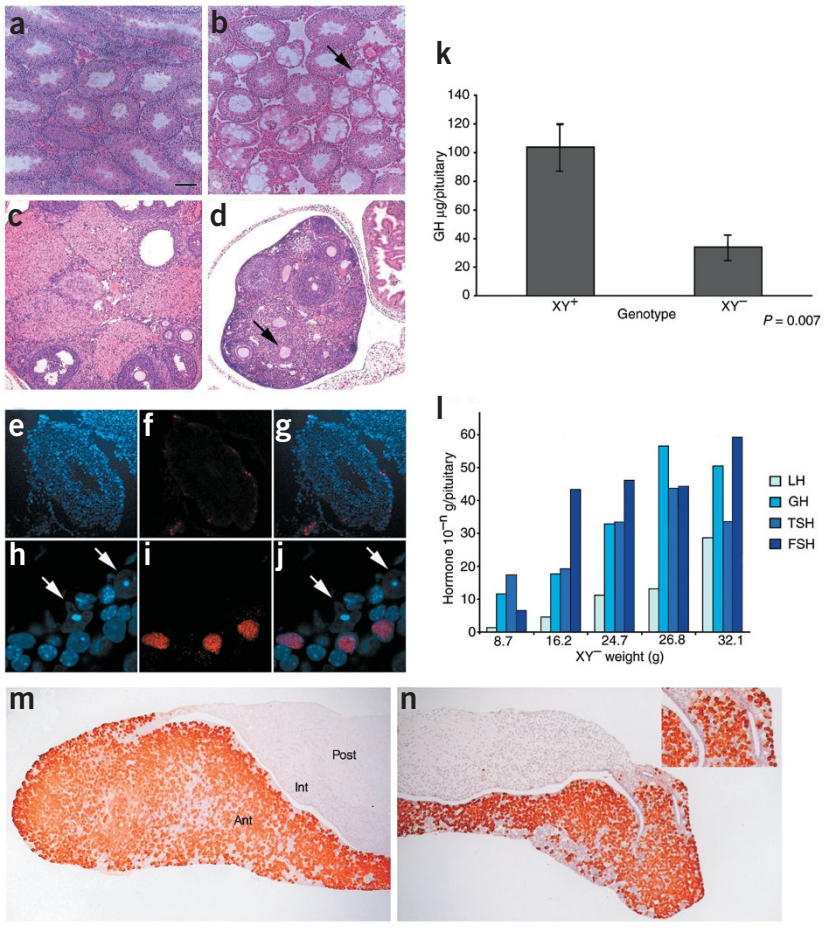

Figure 3 Gonadal histology, pituitary hormone levels and growth hormone immunohistochemistry. (**a**,**b**) Sections through testes of 2.5-month-old wild-type (**a**) and *Sox3*-null males (**b**). Empty, necrotic tubules were present in the mutant (arrow). (**c**,**d**) Sections through ovaries of 2.5-month-old wild-type and mutant females. Some atretic oocytes were present (arrow). (**e**–**j**) SOX3 immunofluorescence on testis sections of a 4-week-old wild-type mouse. (**e**) DAPI staining of a tubule. (**f**) *Sox3* staining. (**g**) Merged image. (**h**) DAPI staining on a confocal image at high magnification. Sertoli cells are easily recognizable by the presence of distinct nucleoli (arrows). (**i**) SOX3 staining. (**j**) Merged image showing the presence of SOX3 in germ cells. (**k**) Growth hormone radioimmunoassay on pituitary protein extracts from seven wild-type (XY^{+}) and five *Sox3*-null (XY^{-}) 2-month-old littermates. (**l**) Relationship between concentrations of luteinizing hormone (LH), FSH, growth hormone (GH) and TSH and body weight in five *Sox3*-null mutant mice. Concentrations on the *y* axis: luteinizing hormone, 10^{-7} g per pituitary; growth hormone, 10^{-6} g per pituitary; TSH, 10^{-8} g per pituitary; FSH, 10^{-8} g per pituitary. (**m**,**n**) Immunohistochemistry for growth hormone on pituitary sections from 6-week-old wild-type and *Sox3* mutant males. The inset in **n** shows an extra cleft containing cells positive for growth hormone. Ant, anterior lobe; Int, intermediate lobe; Post, posterior lobe.

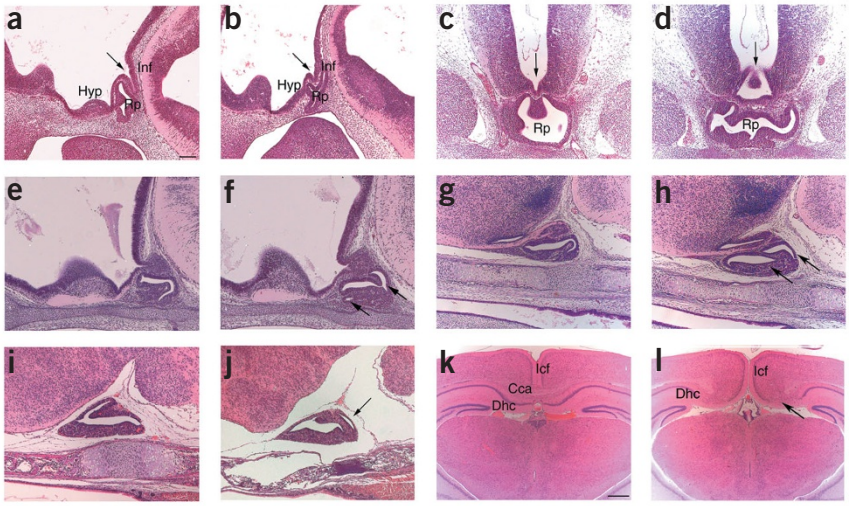

Figure 4 Abnormal morphogenesis of the hypothalamus, pituitary and midline CNS structures in *Sox3* mutant mice. (**a**,**b**) Sagittal sections through the brains of 11.5-d.p.c. wild-type (**a**) and *Sox3*-null embryos (**b**). In the mutant, Rathke's pouch was dorsally expanded and bifurcated and the evagination of the infundibulum was less pronounced (arrow). (**c**,**d**) Coronal sections through the brains of 12.5-d.p.c. wild-type (**c**) and *Sox3*-null embryos (**d**). The morphology of the ventral hypothalamus and infundibulum (arrow) was abnormal in the mutant. (**e**,**f**) Sagittal sections though the brains of 14.5-d.p.c. wild-type (**e**) and *Sox3*-null embryos (**f**). An extra Rathke's pouch lumen was present in the mutant (arrows). (**g**,**h**) Sagittal sections though the brains of 16.5-d.p.c. wild-type (**g**) and *Sox3*-null embryos (**h**), confirming the persistence of an extra Rathke's pouch lumen in the mutant (arrows). (**i**,**j**) Sagittal sections through the heads of newborn wild-type (**i**) and *Sox3*-null (**j**) littermates. An extra lumen and cleft in Rathke's pouch was present in the mutant (arrow). (**k**,**l**) Transverse section through the brains of 3-week-old wild-type and *Sox3* mutant littermates, showing dysgenesis of the corpus callosum in the mutant (arrows). Rp, Rathke's pouch; Inf, infundibulum; Hyp, presumptive hypothalamus; Cca, corpus callosum; Dhc, dorsal hippocampal commissure; Icf, intercerebral fissure. Scale bars: **a** (for **a**–**j**), 0.1 mm; **k** (for **k**,**l**), 0.5 mm.

remnant of the lumen of Rathke's pouch (**Fig. 3m**). In the *Sox3* mutants (**Fig. 3n**), the anterior lobe was much smaller and the distinction between anterior and intermediate pituitary tissue was disrupted on one side by the presence of a second Rathke's cleft structure delineated by typical columnar lining cells. Between these clefts, an aberrant region contained growth hormone–positive anterior lobe cells mingling with intermediate lobe cells.

We then examined pituitary development in the *Sox3* mutants. A sagittal section through the brains of wild-type embryos at 11.5 d.p.c. showed the typical structure of Rathke's pouch overlain by the

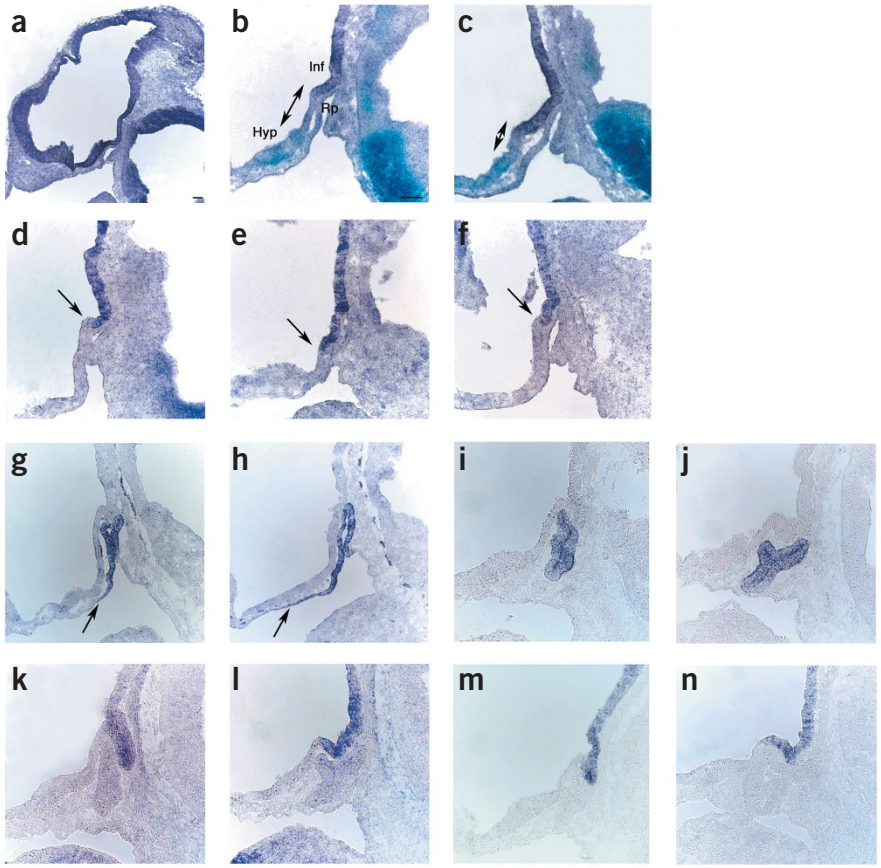

Figure 5 Altered domains of expression of *Fgf8* and *Bmp4* during early development of the pituitary in *Sox3* mutants. (**a**) Sagittal section of a 10.5-d.p.c. wild-type embryo hybridized to *Sox3*. (**b**,**c**) Sagittal sections of 10.5-d.p.c. wild-type (**b**) and *Sox3*-null (**c**) embryos hybridized to *Bmp4* (purple staining) and *Isl1* (blue staining). In the mutant (**c**), the *Bmp4* expression domain was expanded ventrally and fused to the more ventral *Isl1* domain (compare double-headed arrows in **b** and **c**). (**d**–**f**) Sagittal sections of 10.5-d.p.c. wild-type (**d**) and *Sox3*-null (**e**,**f**) embryos hybridized to *Fgf8*. *Fgf8* expression in the infundibulum (arrows) was expanded ventrally in the mutants (**e**,**f**). The extent of this extra *Fgf8* expression domain correlated negatively with infundibular evagination (compare **e** and **f**). (**g**,**h**) Sagittal sections of 10.5-d.p.c. wild-type (**g**) and *Sox3*-null (**h**) embryos hybridized to *Hesx1*, showing an expansion of its expression domain (arrow) in the mutant Rathke's pouch (**h**). (**i**,**j**) Sagittal sections of 11.5-d.p.c. wild-type (**i**) and *Sox3*-null (**j**) embryos hybridized to *Hesx1*. *Hesx1* was expressed in the bifurcated pouch in the mutant (**j**). (**k**,**l**) Sagittal sections of 11.5-d.p.c. wild-type (**k**) and *Sox3*-null (**l**) embryos hybridized to *Bmp4*. At this stage, the expression of *Bmp4* in the mutant was more restricted dorsally than at 10.5 d.p.c. (**m**,**n**) Sagittal sections of 11.5-d.p.c. wild-type (**m**) and *Sox3*-null (**n**) embryos hybridized to *Fgf8*. Like *Bmp4*, *Fgf8* expression in the mutant (**n**) was more dorsally restricted in the abnormal infundibulum. Rp, Rathke's pouch; Inf, infundibulum; Hyp, presumptive hypothalamus. Scale bars: **a**,**b**, (for **b**–**n**), 0.1 mm

infundibulum and the more anterior presumptive hypothalamus (**Fig. 4a**). In contrast, the pouch was expanded and bifurcated in mutant littermates (**Fig. 4b**). The evagination of the infundibulum was much less pronounced, and the presumptive hypothalamus appeared thinner and shorter in mutant embryos. All six mutant embryos sectioned and analyzed in this way had these defects to variable extents. Coronal sections from mutant mice at 12.5 d.p.c. showed that the floor plate of the diencephalon was markedly expanded relative to the typical V shape seen in wild-type embryos in the region overlying the distended bifurcated Rathke's pouch (**Fig. 4c**,**d**). Sections from mice at 14.5 d.p.c. (**Fig. 4e**,**f**) and 16.5 d.p.c. (**Fig. 4g**,**h**) showed the presence of extra Rathke's lumens, presumably originating from the bifurcated pouch, in mutant mice.

All three pituitary lobe tissues were present in mutant mice at birth, but extra Rathke's clefts and lining cells were evident (**Fig. 4i**,**j**). We also observed additional midline CNS abnormalities in the most severely affected mice, including dysgenesis of the corpus callosum, failure of the dorsal hippocampal commissure to cross the midline and apparent continuity of the intercerebral fissure with the third ventricle (**Fig. 4k**,**l**).

Altered expression of *Fgf8* and *Bmp4*

Sox3 was not expressed in Rathke's pouch (**Fig. 5a**) but was present throughout the CNS and, notably, at high levels in the ventral diencephalon, including the infundibulum (**Fig. 5a**). The observed defects in the Rathke's pouch are probably a secondary consequence of the absence of *Sox3* in this domain. We then looked at the expression of *Bmp4* and *Fgf8* in the infundibulum, two genes encoding secreted factors required for the development of Rathke's pouch[3,4].

We examined embryos at 10.5 d.p.c., 24 h before any morphological defect became apparent in Rathke's pouch in the *Sox3* mutants. In the wild-type control (**Fig. 5d**), *Fgf8* expression was limited to the infundibulum overlying the dorsal edge of Rathke's pouch. In contrast, *Sox3* mutants showed *Fgf8* expression in an expanded ventral territory (**Fig. 5e**,**f**). The extent of this territory varied among the mutant embryos and correlated negatively with infundibular evagination: the greater the infundibular evagination, the less the ventral expansion of *Fgf8* expression (compare **Fig. 5e** and **f**). The expansion of *Fgf8* expression could reflect the aberrant morphology of the infundibulum (**Fig. 3**) or a more general defect in the ventral diencephalon. We therefore decided to compare the expression of another infundibular marker, *Bmp4*, with that of a more ventral, presumptive hypothalamic one, *Isl1* (ref. 19) using double *in situ* hybridization. In sections from control mice (**Fig. 5b**), as for *Fgf8*, expression of *Bmp4* was restricted to the infundibulum above Rathke's pouch, whereas *Isl1* was present more ventrally, overlying the oral ectoderm. Mutant mice showed an expansion of the *Bmp4* expression domain, such that it was in direct contact with the *Isl1* expression territory (**Fig. 5c**). This result suggests that the expansion of *Bmp4* and *Fgf8* could be the result of ectopic expression. This expansion was only transient, because the expression of the two molecules was restricted more dorsally in *Sox3*-null embryos at 11.5 d.p.c., by which time the morphological defects were obvious (**Fig. 5k–n**).

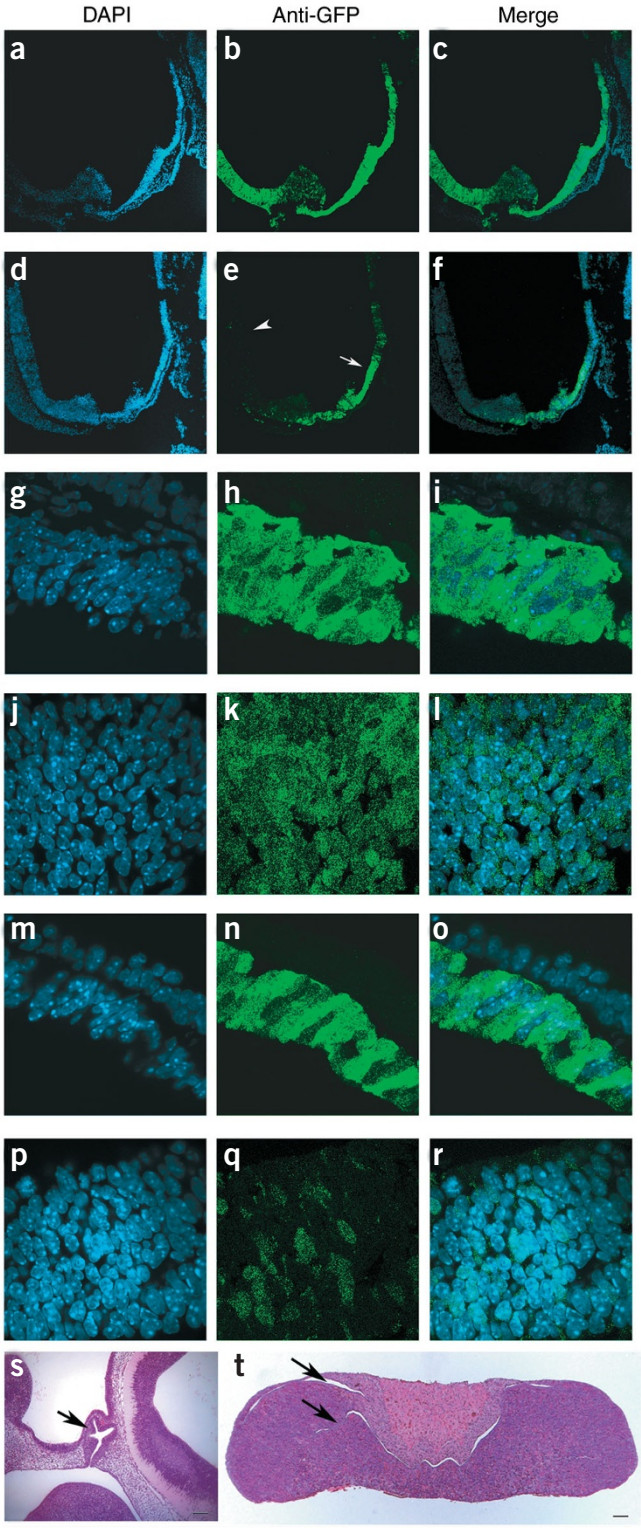

Figure 6 GFP expression from *Sox3*$^{\Delta gfp}$ in XY hemizygous and XX heterozygous embryos and pituitary defects in heterozygotes. (**a**–**f**) Confocal imaging of GFP immunofluorescence on sagittal sections of 10.5-d.p.c. *Sox3*-null (**a**–**c**) and heterozygous (**d**–**f**) embryos. (**g**–**r**) High-magnification confocal imaging of two regions of the same sections. (**g**–**i**,**m**–**o**) Images through the infundibulum and hypothalamic region (corresponding to the white arrow in **e**) of *Sox3*-null (**g**–**i**) and heterozygous (**m**–**o**) embryos. (**j**–**l**,**p**–**r**) Images through the forebrain (region corresponding to the white arrowhead in **e**) of *Sox3*-null (**j**–**l**) and heterozygous (**p**–**r**) embryos. In the *Sox3*-null embryos, the infundibulum, hypothalamic and forebrain regions were uniformly stained for GFP (compare **h** and **k**), whereas in *Sox3* heterozygotes, GFP expression was mosaic in the forebrain region but uniformly bright in the infundibulum and hypothalamic region (compare **q** and **n**). (**s**) Sagittal section through the brain of an 11.5-d.p.c. heterozygous embryo. Rathke's pouch was expanded and bifurcated (arrow). (**t**) Transverse section through the pituitary gland of a 3-month-old heterozygous female showing the presence of extra clefts (arrows). Scale bars, 0.1 mm.

This transient expansion of the domain responsible for inducing Rathke's pouch would be expected to have molecular consequences in the responding tissue. We therefore looked at the expression of the transcription factor *Hesx1*, whose expression is restricted to Rathke's pouch at 10.5 d.p.c. (ref. 20; **Fig. 5g**). In mutant mice (**Fig. 5h**), the *Hesx1* expression domain was expanded anteriorly. After separation from the oral ectoderm at 11.5 d.p.c., *Hesx1* was expressed throughout Rathke's pouch in wild-type mice (**Fig. 5i**) and in the bifurcated pouch in mutant mice (**Fig. 5j**).

Mosaic analysis in XX *Sox3*$^{\Delta gfp}$ heterozygous embryos

Despite the widespread expression of *Sox3* in the CNS, the main defects observed in mutant embryos were restricted to specific territories. Are these territories more sensitive to subtle modifications that did not cause obvious defects elsewhere, or does this phenomenon reflect a particular requirement for SOX3 in specific regions? Because *Sox3* is X-linked and only one copy of the X chromosome is active in somatic cells[20], XX embryos heterozygous with respect to *Sox3*$^{\Delta gfp}$ should have mosaic expression of the wild-type and mutated alleles. Such mosaicism should be reflected in the activity of the GFP reporter in territories where *Sox3* is normally expressed. Any nonrandom distribution of GFP-positive cells would indicate differences in properties between cells expressing *Sox3* and those not expressing *Sox3*.

We first assessed the distribution of GFP immunofluorescence in *Sox3*-null embryos at 10.5 d.p.c. (**Fig. 6a**,**c**). As expected, all cells in the CNS were GFP positive and the infundibulum and hypothalamic region had an intense signal (**Fig. 6b**). In heterozygous ($XX^{+/-}$) embryos (**Fig. 6d**,**f**), we observed a bright, seemingly homogenous GFP-positive region (**Fig. 6e**) in this territory, whereas the rest of the CNS had the speckled pattern expected from a mosaic X-inactivated allele (**Fig. 6e**). Examination of higher magnification, confocal sections confirmed the ubiquitous expression of GFP in the *Sox3*-null embryos (**Fig. 6g**,**l**), both in the infundibulum and hypothalamic region (**Fig. 6g–i**) and in the forebrain (**Fig. 6j–l**). They also showed that GFP-positive, *Sox3*-negative cells were the main, if not only, cells present in the infundibulum and hypothalamic region of heterozygous embryos ($n = 8$; **Fig. 6m–r**). Examination of heterozygotes at later stages showed that this GFP-positive domain persisted, such that by 15.5 d.p.c. it was present in the hypothalamus and infundibulum (**Supplementary Fig. 2** online).

The presence of the GFP-positive patch at 10.5 d.p.c. confirmed that there is a specific requirement for *Sox3* in the infundibulum and hypothalamic region. Furthermore, if aberrant signaling from this region is responsible for the morphological abnormalities of Rathke's pouch in null embryos, then $XX^{+/-}$ embryos should also have a bifurcated Rathke's pouch, as signaling from this coherent patch of *Sox3*-negative cells should be similarly abnormal. Histological analysis of embryos at 11.5 d.p.c. confirmed the presence of a bifurcated Rathke's pouch in three of four heterozygous embryos. Moreover, three of four adult $XX^{+/-}$ mice had abnormal pituitary morphology (**Fig. 6s**,**t**), similar to that seen in null mice, suggesting that the patch of *Sox3*-negative, GFP-positive cells was responsible for inducing the dysmorphic Rathke's pouch.

The nonrandom distribution of GFP-positive cells could be due to altered rates of cell proliferation. We therefore used 5-bromodeoxyuridine (BrdU) to label dividing cells at 10.5 d.p.c. Very few cells in the GFP-positive patch in heterozygotes showed BrdU staining compared with cells outside this region (**Fig. 7**). This was not seen in wild-type controls. We counted the number of $BrdU^+$ cells in two restricted areas, in the GFP-positive patch and adjacent to this in the CNS, in heterozygous embryos and in equivalent regions in controls. In the wild-type controls ($n = 5$), the distribution of $BrdU^+$ cells was homogeneous across the infundibulum and hypothalamic region with 47.6% of $BrdU^+$ cells located in the region corresponding to the patch, whereas in heterozygous embryos ($n = 4$), only 23.6% of the $BrdU^+$ cells were located in the GFP-positive patch (mean ± s.e. for angular transformation: wild-type, 43.6 ± 1.6%; heterozygotes, 29.1 ± 3.43%; $P < 0.005$). The percentage of $BrdU^+$ cells outside the patch in mutant embryos was similar to that in controls, indicating that proliferation was reduced by a factor of ~3 within the GFP-positive patch. By TUNEL assay, we observed no differences in the cell death patterns in the GFP-positive domain in heterozygous and wild-type embryos (**Supplementary Fig. 3** online). These results confirm that within this domain, cells lacking SOX3 have properties different from those with SOX3 and indicate that the protein is necessary to maintain normal rates of proliferation in this population of neuroepithelial precursors.

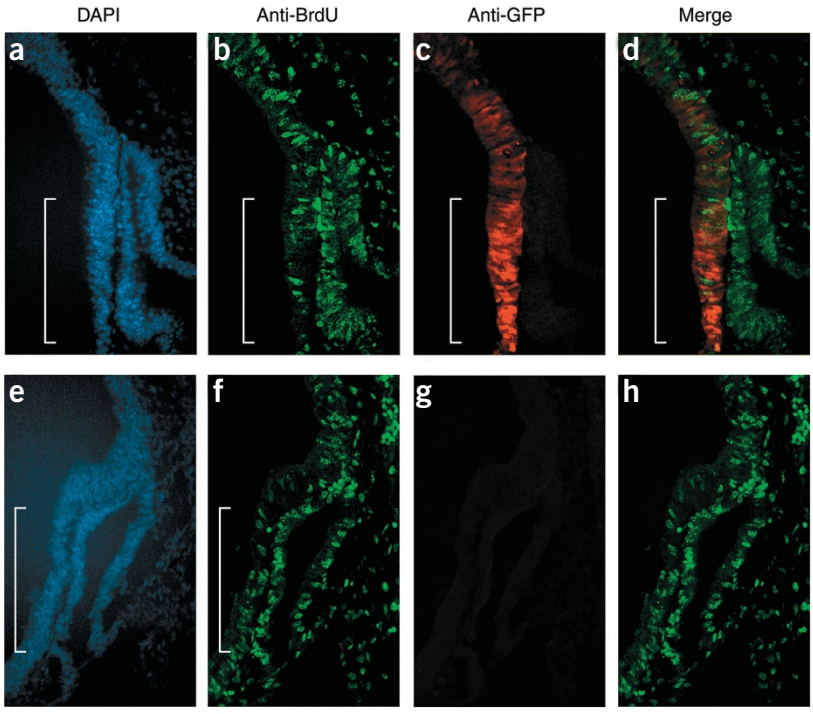

Figure 7 Proliferation in the infundibulum and hypothalamic region of XX heterozygous *Sox3*$^{\Delta gfp}$ embryos. (**a**–**d**) BrdU staining and GFP expression in the infundibulum and hypothalamic region of a 10.5-d.p.c. heterozygous ($XX^{+/-}$) *Sox3*$^{\Delta gfp}$ embryo. In the GFP-positive patch (bracket), few cells showed BrdU staining compared with cells outside this region. (**e**–**h**) BrdU staining in a corresponding domain (bracket) of the infundibulum and hypothalamic region of a wild-type embryo showed a homogenous BrdU staining pattern.

Sox3 expression persists in the postnatal hypothalamus

Although heterozygotes had morphological abnormalities in Rathke's pouch (**Figs. 3n** and **6t**), there were no phenotypic defects with respect to growth or fertility, and concentrations of pituitary growth hormone in 2-month-old heterozygotes were similar to those in wild-type littermates (40.9 ± 4.1 versus 39.1 ± 4.8 g growth hormone per pituitary, respectively; $n = 7$ per group). This could be because the defects in Rathke's pouch were less severe in the heterozygotes or because there were additional defects in the null mice. Production of pituitary growth hormone is controlled by hypothalamic trophic factors, but these effects are mostly manifested postnatally[21,22]. Therefore, to assess whether the morphological defects compromised pituitary function before hypothalamic input, we measured growth hormone levels at 18.5 d.p.c. and found these to be identical (3.5 ± 0.04 g) in pituitary extracts from mutants ($n = 5$) and wild-type littermates ($n = 9$). Therefore, there must be additional defects in the null mice, probably at the level of hypothalamic control.

We therefore carried out histological examination of the mature hypothalamus. In sections from wild-type mice (**Fig. 8a**), the cellular densities corresponding to several nuclei (*e.g.*, paraventricular or arcuate (ARC)) were visible. These were recognizable in the *Sox3* mutant mice (**Fig. 8b**) with no obvious abnormalities, although the general cellular density was slightly reduced in medial regions of the hypothalamus. We also examined the hypothalamic ARC–median eminence region for GFP expression postnatally. We observed abundant GFP-positive cells throughout the ARC, including the ventrolateral zones, in the *Sox3* mutants (**Fig. 8c**,**d**). At higher magnification, GFP could be seen in cell bodies and in axon projections throughout the median eminence (**Fig. 8d**). GFP-positive cells also delineated the ependymal lining of the third ventricle. We observed similar expression in wild-type brains by *in situ* hybridization for *Sox3* (data not shown).

DISCUSSION

Mice with a deletion of *Sox3* have pleiotropic phenotypes, including craniofacial abnormalities, midline CNS defects and hypopituitarism. We show that *Sox3* activity is required in the ventral diencephalon for morphogenesis and differentiation of the infundibulum and hypothalamus and to correctly induce the morphogenesis of Rathke's pouch. Although pituitary development is abnormal in *Sox3*-null mice, this may not in itself be sufficient to explain the hypopituitarism, which is probably due to additional defects at the level of hypothalamic control. We observed a slight reduction in the number of cells in the hypothalamus, but the lack of SOX3 could also compromise the function of specific neurons in the ARC, in which its expression is normally maintained, without having much effect on their survival. The ventral ARC–median eminence region also selectively maintains $Sox3^{\Delta gfp}$ expression. As the primary role of this structure is to convey signals from the hypothalamus to the pituitary, a *Sox3*-dependent deficit in this region could make a continuing contribution to the dysfunction of an abnormal pituitary.

There is wide variation in the severity of phenotypes in *Sox3*-null mice, for which there are at least two explanations. First, there is variation due to their mixed genetic background. Fewer mice were born as we backcrossed the *Δgfp* mutation onto the 129sv/ev strain, suggesting that some were lost at embryonic stages (data not shown). This is consistent with our previous studies in which *Sox3*-null 129sv/ev XY ES cells generated chimeras that died from gastrulation defects (M. Parsons, C. Wise, S.B., M. Cohen-Tannoudji, K.R., L. Pevny & R.L.-B., unpublished data).

Second, SOX3 has a largely indirect effect on pituitary morphogenesis: development of Rathke's pouch is disrupted despite *Sox3* not being expressed in the pouch. Thus, the primary defect in the $Sox3^{\Delta gfp}$ mutants must lie in the inducing tissues of the ventral diencephalon, as shown by the flattened morphology and expanded domains of *Bmp4* and *Fgf8* expression. The defects in Rathke's pouch are almost certainly due to overinduction, as they are similar to, though less severe than, those observed when FGF8 was expressed ectopically in Rathke's pouch[4]. Other inducing molecules may also be involved. Supporting the overinduction explanation, the expression domain of the homeobox gene *Hesx1* in this domain was expanded at the same time. Similar Rathke's pouch phenotypes have been reported in mice with a deletion of *Hesx1*, and mutations of the homolog in humans are responsible for some cases of septo-optic dysplasia[23]. But *Hesx1* is also expressed earlier, during the formation of the prospective forebrain, and so its absence from the CNS may be indirectly responsible for the malformed Rathke's pouch, as shown for *Sox3*.

An independent *Sox3* mutation in mice results in a similarly variable phenotype[24], which included defects in growth, craniofacial development and fertility, similar to our results described here. But the authors did not report any pituitary abnormalities, focusing instead on the gonadal abnormalities. With respect to the latter, they concluded that SOX3 was expressed in Sertoli cells, and we interpret their data to be consistent with ours, which shows that the protein is found in spermatogonia.

The three *Soxb1* genes are expressed in neuroepithelial progenitor and stem cells from the earliest stages. Some direct evidence that they are

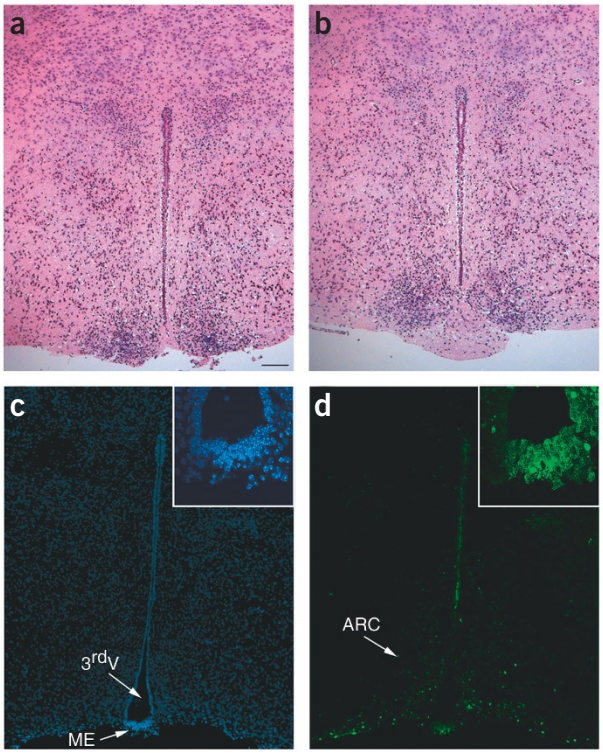

Figure 8 Histological analysis and GFP immunofluorescence of the hypothalamus in the postnatal brain of *Sox3* mutants. (**a**,**b**) Transverse sections through the hypothalamus of postnatal day 5 (P5) wild-type (**a**) and *Sox3*-null (**b**) male littermates. The general cellular density was reduced in the mutant. (**c**,**d**) Detection of GFP expression by immunofluorescence on a transverse section through the hypothalamus of a P3 *Sox3*-null mouse. DAPI image (**c**) and GFP immunofluorescence (**d**) were present throughout the ARC. Confocal high-magnification images of the median eminence (ME; insets in **c** and **d**) showed GFP staining throughout the median eminence. 3rdV, third ventricle.

involved in neuroectoderm induction and maintenance has come from studies in fruit flies, frogs and chicks[25,26], suggesting that mutations in *Soxb1* genes in mice will probably affect the formation of the CNS.

The lack of SOX3 led to dysgenesis of the corpus callosum, but the infundibulum and prospective hypothalamus were present, although they were thinner and flatter. Because SOX1 and SOX2 continued to be expressed, any effects were likely to be subtle. We therefore examined XX $Sox3^{\Delta gfp}$ heterozygotes, taking advantage of X inactivation to compare the properties of cells expressing the wild-type *Sox3* allele with those of cells expressing $Sox3^{\Delta gfp}$ within the same embryo.

We expected that cells expressing the mutated allele might be competed out in areas where SOX3 function is crucial, especially if cell proliferation was compromised. But we observed a patch of *Sox3*-negative, GFP-positive cells specifically in the region of the infundibulum and presumptive hypothalamus. Overproliferation could explain an apparent coherent patch, but in fact these cells had a marked reduction in proliferation, consistent with the association of *Soxb1* gene activity in dividing neuroepithelial cells. Alternatively, cells expressing *Sox3* could preferentially differentiate and migrate away or the lack of *Sox3* could alter the adhesive properties of cells in this region. We looked at some neuronal differentiation markers (N-cadherin, *Hes5* and *Mash1*) but observed no obvious precocious differentiation of cells throughout the region (data not shown). The remaining explanation is that the cells in the GFP-positive patch have properties that promote their separation from surrounding cells expressing *Sox3*.

The reduction in proliferation provides a simple explanation for the failure of the infundibulum to fully evaginate and for the subsequent flattening and stretching of the region that also includes the prospective hypothalamus. This may account in part for the enlarged domains of *Fgf8* and *Bmp4* expression and could explain the presence of a shorter interval between the apparently expanded infundibulum and the *Isl1*-positive presumptive hypothalamus. Although we used *Isl1* expression as a landmark, however, it is conceivable that the lack of SOX3 led to an expansion of its normal territory. There could be a more general alteration in rostral-caudal patterning in this region.

The abundance of *Sox3* expression in a group of ventral hypothalamic cells and the median eminence postnatally is notable, as these structures are implicated in the control of pituitary function. The distribution of GFP-positive cells does not suggest restriction to any single type of neuroendocrine cell. But the ventrolateral distribution of GFP-positive cells overlaps that of growth hormone–releasing hormone cells, whose product directly regulates secretion of pituitary growth hormone[27]. Compromise of the number, connectivity or activity of growth hormone–releasing hormone cells in the absence of SOX3 postnatally would cause functional growth hormone deficiency. GFP-positive cells were scattered in the hypothalamus of heterozygotes, unlike the clustering pattern seen in the posterior pituitary, and so the cells expressing SOX3 are probably sufficient to achieve normal pituitary function.

The hypopituitary phenotype of the *Sox3*-null mice resembles that described for humans with an 11-mer polyalanine tract expansion in *SOX3*. Some of these individuals also have craniofacial abnormalities that could relate to those in the mutant mice[6]. Another group of individuals with X-linked hypopituitarism have duplications of the chromosomic region including *SOX3*, and their phenotype is probably due to overexpression of the gene[28]. As these individuals do not have craniofacial defects, the polyalanine tract expansion is probably a loss-of-function mutation. The wide phenotypic variation of *Sox3* mutant mice is also evident in both sets of affected humans. Presumably, as in the mice, this variation is due to a combination of genetic background effects and the indirect nature of the final phenotype.

Our results have several other implications for hypopituitarism in humans. If both gain- and loss-of-function mutations can lead to hypopituitarism, then pituitary development must be very sensitive to SOX3 dosage. *SOX3* should therefore be considered a good candidate, not only for association with X-linked inheritance, but also for sporadic cases of hypopituitarism. As these are more prevalent in boys than girls[29], *SOX3* may be a good candidate for unexplained hypopituitarism in boys. Our studies in mice also highlight the potential involvement of hypothalamic abnormalities in *Sox3* mutants, in addition to their pituitary dysmorphogenesis. This may be difficult to detect with magnetic resonance imaging in individuals with *SOX3* mutations, although some of these individuals have an ectopic posterior pituitary (P.Q.T., unpublished data; M. Dattani, personal communication). Because the severity of the phenotype is so variable in mice, the expected phenotype for humans with *SOX3* mutations could be quite broad, ranging from mild growth hormone deficiency to severe panhypopituitarism with CNS midline abnormalities. Examination of such individuals might also identify other CNS midline defects, as noted in the mutant mice. Moreover, we would predict that apparently healthy mothers of affected XY offspring are likely to have abnormal Rathke's pouch derivatives, even if this is not reflected in overt hormone deficiencies.

METHODS

Targeting constructs, ES cell transfection and germline transmission. The targeting vector was based on a 7.5-kb *Eco*RI-*Bgl*II fragment of genomic *Sox3* (**Fig. 1a**). We inserted a *lox*P site at the *Xho*I site, downstream of the TATA box, creating an additional *Xmn*I site in the locus. We cloned the GFP coding sequence, a gift from M. Zernicka-Goetz[14] (Wellcome Trust/Cancer UK Gurdon Institute of Cancer and Developmental Biology, Cambridge, UK) downstream of a *lox*P site and upstream of an SV40 polyA site. We placed the *pgk-neo*^{r} cassette between two direct FRT sequences in the FRT2 vector[30]. We then cloned this sequence downstream of the GFP coding sequence in the *lox*P-GFP construct, in opposite transcriptional orientation, creating the final selection cassette. We introduced this cassette into the *Spe*I site of the previously modified genomic fragment, downstream of the *Sox3* polyA sequence. Both *lox*P sites are in the same orientation.

We electroporated the targeting vector into AB1 XY ES cells[31], derived from the black agouti 129sv/ev mouse strain. We screened 500 G418-resistant clones by Southern blotting. We identified correctly targeted ES cell clones by the presence of *Bgl*II fragments of 7.5 kb instead of 9 kb (**Fig. 1b**), by the presence of *Bgl*II-*Xmn*I fragments of 3.5 kb instead of 4 kb and by the presence of *Bam*HI fragments of 14 kb instead of 11 kb (data not shown). Five ES clones carried the $Sox3^{neo}$ floxed allele. The sequences of the primers used for genotyping are available on request.

Generation and analysis of chimeric embryos. We injected targeted ES cells into 3.5-d.p.c. C57BL/6 (B6) blastocysts and transferred them into 2.5-d.p.c. CBA C57BL/10 pseudopregnant mothers. We obtained high-percentage chimeras (70–100% agouti pigmentation) for all the $Sox3^{flox.gfp}$ clones. Male chimeras were bred to MF1 females, and their agouti pups were genotyped to confirm germline transmission of the targeted allele (**Fig. 1**). We confirmed germline transmission of the targeted allele in offspring from two targeted ES cell clones.

Mice. We maintained the *Sox3* conditional mutation on MF1 (random bred) and 129SvEv inbred backgrounds (NIMR). The β-actin–Cre line[15] was maintained on a MF1 background and was used to obtain the *Sox3* deleted allele ($Sox3^{\Delta gfp}$) in embryos and mice. We obtained fertile hemizygous male (XY^-) and heterozygous females ($XX^{+/-}$) directly in this way, on a largely MF1 outbred background, and then bred them to derive embryos and mice carrying the $Sox3^{\Delta gfp}$ allele. The selection cassette was present in the mice used in this study. We carried out all mouse experiments using protocols approved under the UK Animal (scientific procedures) Act.

Histology, *in situ* hybridization and immunofluorescence. For histology, we fixed embryos in Bouin's, dehydrated them through graded ethanol series and embedded them in paraffin. We stained sections with hematoxylin and eosin as described[32]. We carried out whole-mount *in situ* hybridization of embryos as described[33]. We carried out single and double *in situ* hybridization on frozen sections as described[34], using *Sox3* (ref. 35), *Bmp4* (ref. 36) *Fgf8* (ref. 37) and *Isl1* (ref. 19) probes. For frozen sections, we fixed the embryos in 4% paraformaldehyde for up to 2 h at 4 °C, cryoprotected them in 20% sucrose and embedded them in OCT (BDH). We analyzed immunofluorescence on 12- m frozen sections as described[38] using a 1:1,000 dilution of an antibody to GFP (Molecular Probes) and a 1:500 dilution of a goat antibody to rabbit conjugated to Alexa-488 or Alexa-594 (Molecular Probes). Confocal images were obtained using a Leica TCS SP microscope and TCSNT software.

Radioimmunoassay and growth hormone immunohistochemistry. We homogenized anterior pituitary glands in phosphate-buffered saline and assayed them for growth hormone, luteinizing hormone, FSH and TSH by specific radioimmunoassays using NHPP reagents provided by A.F. Parlow (National Hormone & Peptide Program, Torrance, California, USA). For growth hormone immunohistochemistry, we used a 1:2,000 dilution of a monkey antibody to rat growth hormone serum from the NHPP as previously described[39].

BrdU incorporation. We injected pregnant females intraperitoneally with 100 g of BrdU (Sigma) per g of body weight and killed them after 1 h. We processed embryos as described above for immunofluorescence. After 30 min post-fixation in 4% paraformaldehyde, we incubated sections for 1 min in 0.05% pepsin (Sigma) in 0.01 N HCl at 37 °C. BrdU labeling was exposed by a 30-min treatment with 2 N HCl at 37 °C, neutralized by three washes in 0.1 M Borate, pH 8.5. We then incubated sections overnight at 4 °C with a 1:100 dilution of a fluorescein-conjugated monoclonal antibody to BrdU (Boehringer Mannheim). Under the conditions used for the BrdU staining, GFP fluorescence was undetectable. We counted $BrdU^+$ cells by selecting a square that fit the narrowest part of the region to be examined and counting $BrdU^+$ cells inside this square. We did this five times per section in each of the two areas to be examined, inside a region corresponding to the GFP-positive patch and directly above it. We counted one section for each embryo and calculated the percentage of proliferating cells in the GFP-positive patch. After angular transformation of the percentages[40], we estimated the significance of the difference in proliferation between the two genotypes using Student's *t*-test.

Note: Supplementary information is available on the Nature Genetics website.

ACKNOWLEDGMENTS

We thank I. Harragan and W. Hatton for assistance with histology, J. Turner and P. Burgoyne for sharing their expertise in gonadal phenotypes, D. Whittcut and P. Mealyer for taking good care of the mouse colony, L. Dubois and J.-P. Vincent for critical reading of the manuscript and C. Wise and other members of the laboratory for their help and encouragement. This work was supported by the MRC, by a European Union Network Grant and the Louis Jeantet Foundation and by Marie Curie Postdoctoral Fellowships to K.R. and S.B.

COMPETING INTERESTS STATEMENT

The authors declare that they have no competing financial interests.

Received 1 December 2003; accepted 26 January 2004
Published online at http://www.nature.com/naturegenetics/

1. Dasen, J.S. & Rosenfeld, M.G. Signaling and transcriptional mechanisms in pituitary development. *Annu. Rev. Neurosci.* **24**, 327–355 (2001).
2. Kimura, S. *et al.* The T/ebp null mouse: thyroid-specific enhancer-binding protein is essential for the organogenesis of the thyroid, lung, ventral forebrain, and pituitary. *Genes Dev.* **10**, 60–69 (1996).
3. Ericson, J., Norlin, S., Jessell, T.M. & Edlund, T. Integrated FGF and BMP signaling controls the progression of progenitor cell differentiation and the emergence of pattern in the embryonic anterior pituitary. *Development* **125**, 1005–1015 (1998).
4. Treier, M. *et al.* Multistep signaling requirements for pituitary organogenesis in vivo. *Genes Dev.* **12**, 1691–1704 (1998).
5. Schepers, G.E., Teasdale, R.D. & Koopman, P. Twenty pairs of sox: extent, homology, and nomenclature of the mouse and human sox transcription factor gene families. *Dev. Cell* **3**, 167–170 (2002).
6. Laumonnier, F. *et al.* Transcription factor SOX3 is involved in X-linked mental retardation with growth hormone deficiency. *Am. J. Hum. Genet.* **71**, 1450–1455 (2002).
7. Stevanovic, M., Lovell-Badge, R., Collignon, J. & Goodfellow, P.N. SOX3 is an X-linked gene related to SRY. *Hum. Mol. Genet.* **2**, 2013–2018 (1993).
8. Zucchi, I. *et al.* Transcription map of Xq27: candidates for several X-linked diseases. *Genomics* **57**, 209–218 (1999).
9. Collignon, J. Study of a new family of genes related to the mammalian testis determining gene. (University of London, 1992).
10. Foster, J.W. & Graves, J.A. An SRY-related sequence on the marsupial X chromosome: implications for the evolution of the mammalian testis-determining gene. *Proc. Natl. Acad. Sci. USA* **91**, 1927–1931 (1994).
11. Collignon, J. *et al.* A comparison of the properties of Sox-3 with Sry and two related genes, Sox-1 and Sox-2. *Development* **122**, 509–520 (1996).
12. Wood, H.B. & Episkopou, V. Comparative expression of the mouse Sox1, Sox2 and Sox3 genes from pre-gastrulation to early somite stages. *Mech. Dev.* **86**, 197–201 (1999).
13. Uchikawa, M., Kamachi, Y. & Kondoh, H. Two distinct subgroups of Group B Sox genes for transcriptional activators and repressors: their expression during embryonic organogenesis of the chicken. *Mech. Dev.* **84**, 103–120 (1999).
14. Zernicka-Goetz, M. & Pines, J. Use of Green Fluorescent Protein in mouse embryos. *Methods* **24**, 55–60 (2001).
15. Lewandoski, M., Meyers, E.N. & Martin, G.R. Analysis of Fgf8 gene function in vertebrate development. *Cold Spring Harb. Symp. Quant. Biol.* **62**, 159–168 (1997).
16. Graves, J. Interactions between *SRY* and *SOX* genes in mammalian sex determination. *BioEssays* **20**, 264–269 (1998).
17. Kendall, S.K., Samuelson, L.C., Saunders, T.L., Wood, R.I. & Camper, S.A. Targeted disruption of the pituitary glycoprotein hormone alpha-subunit produces hypogonadal and hypothyroid mice. *Genes Dev.* **9**, 2007–2019 (1995).
18. McGuinness, L. *et al.* Autosomal dominant growth hormone deficiency disrupts secretory vesicles in vitro and in vivo in transgenic mice. *Endocrinology* **144**, 720–731 (2003).
19. Thor, S., Ericson, J., Brannstrom, T. & Edlund, T. The homeodomain LIM protein Isl-1 is expressed in subsets of neurons and endocrine cells in the adult rat. *Neuron* **7**, 881–889 (1991).
20. Avner, P. & Heard, E. X-chromosome inactivation: counting, choice and initiation. *Nat. Rev. Genet.* **2**, 59–67 (2001).
21. Shibusawa, N. *et al.* Requirement of thyrotropin-releasing hormone for the postnatal functions of pituitary thyrotrophs: ontogeny study of congenital tertiary hypothyroidism in mice. *Mol. Endocrinol.* **14**, 137–146 (2000).
22. Lin, S.C. *et al.* Molecular basis of the little mouse phenotype and implications for cell type-specific growth. *Nature* **364**, 208–213 (1993).
23. Dattani, M.T. *et al.* Mutations in the homeobox gene HESX1/Hesx1 associated with septo-optic dysplasia in human and mouse. *Nat. Genet.* **19**, 125–133 (1998).
24. Weiss, J. *et al.* Sox3 is required for gonadal function, but not sex determination, in males and females. *Mol. Cell. Biol.* **23**, 8084–8091 (2003).
25. Overton, P.M., Meadows, L.A., Urban, J. & Russell, S. Evidence for differential and redundant function of the Sox genes Dichaete and SoxN during CNS development in Drosophila. *Development* **129**, 4219–4228 (2002).
26. Uwanogho, D. *et al.* Embryonic expression of the chicken Sox2, Sox3 and Sox11 genes suggests an interactive role in neuronal development. *Mech. Dev.* **49**, 23–36 (1995).
27. Mayo, K.E. *et al.* Regulation of the pituitary somatotroph cell by GHRH and its receptor. *Recent Prog. Horm. Res.* **55**, 237–67 (2000).
28. Solomon, N.M. *et al.* Increased gene dosage at Xq26-q27 is associated with X-linked hypopituitarism. *Genomics* **79**, 553–559 (2002).
29. Lindsay, R., Feldkamp, M., Harris, D., Robertson, J. & Rallison, M. Utah Growth Study: growth standards and the prevalence of growth hormone deficiency. *J. Pediatr.* **125**, 29–35 (1994).
30. Dymecki, S.M. Flp recombinase promotes site-specific DNA recombination in embryonic stem cells and transgenic mice. *Proc. Natl. Acad. Sci. USA* **93**, 6191–6196 (1996).
31. McMahon, A.P. & Bradley, A. The Wnt-1 (int-1) proto-oncogene is required for development of a large region of the mouse brain. *Cell* **62**, 1073–1085 (1990).
32. Kaufman, M.H. *The Atlas of Mouse Development.* (Academic, London, 1994).
33. Avilion, A.A., Bell, D.M. & Lovell-Badge, R. Micro-capillary tube in situ hybridisation: a novel method for processing small individual samples. *Genesis* **27**, 76–80 (2000).
34. Dunwoodie, S.L., Henrique, D., Harrison, S.M. & Beddington, R.S. Mouse Dll3: a novel divergent Delta gene which may complement the function of other Delta homologues during early pattern formation in the mouse embryo. *Development* **124**, 3065–3076 (1997).
35. Parsons, M. A functional analysis of Sox3, an X-linked Sry related gene. (University of London, 1997).
36. Jones, C.M., Lyons, K.M. & Hogan, B.L. Expression of TGF-beta-related genes during mouse embryo whisker morphogenesis. *Ann. NY Acad. Sci.* **642**, 339–345 (1991).
37. Martinez-Barbera, J.P. *et al.* Regionalisation of anterior neuroectoderm and its competence in responding to forebrain and midbrain inducing activities depend on mutual antagonism between OTX2 and GBX2. *Development* **128**, 4789–4800 (2001).
38. Li, M., Pevny, L., Lovell-Badge, R. & Smith, A. Generation of purified neural precursors from embryonic stem cells by lineage selection. *Curr. Biol.* **8**, 971–974 (1998).
39. Flavell, D.M. *et al.* Dominant dwarfism in transgenic rats by targeting human growth hormone (GH) expression to hypothalamic GH-releasing factor neurons. *EMBO J.* **15**, 3871–3879 (1996).
40. Snedecor, G. & Cochran, W. *Statistical Methods.* (1967).